Preparation and Electronic Structure of Substituted Aromatic Dithiolene Complexes of Gold(III)

N. C. Schiødt,[†] P. Sommer-Larsen,[§] T. Bjørnholm,*[,†] M. Folmer Nielsen,[‡] J. Larsen,[†] and K. Bechgaard[†,§]

Centre for Interdisciplinary Studies of Molecular Interactions and Department of Chemistry, SYMBION Science Park, University of Copenhagen, Fruebjergvej 3, DK-2100 Copenhagen, Denmark

Received March 4, 1994[⊗]

Ab initio calculations on the complex ion bis(benzene-1,2-dithiolato)aurate(III), **I**, have been performed and show that the two highest occupied MO's have π-character and correspond to the symmetric and antisymmetric combination of the pure ligand HOMO's with only a very small contribution from gold orbitals. Both ligand and metal orbitals contribute significantly to the LUMO which has σ-character. A series of 10 derivatives of **I** have been prepared and isolated as tetra-*n*-butylammonium salts. The electronic spectra of these species show two symmetry-forbidden transitions in good agreement with calculations. A spectrochemical series is proposed and related to the electron-releasing efficiency of the substituents. Comparison of the potentials for the reversible oxidation of the complexes (measured by cyclic voltammetry) with the energy of the lowest lying electronic transition reveals a linear relationship which is discussed in terms of the degree of charge transfer from ligands to metal. Improved synthesis of some of the ligands is reported.

Introduction

Transition metal dithiolene complexes have been thoroughly investigated because of their vivid redox-behavior and their interesting coordination geometry.[1−7] Dithiolene complexes of gold have been prepared as the green, planar bis complexes of Au(III).[8−11] The monoanionic species can be reduced to paramagnetic dianions[12−15] or oxidized to neutral, radicaloid species.[16−18] Further oxidized species of dithiolene gold complexes have been observed in crystals containing inorganic anions.[19]

Several salts containing transition metal dithiolene complexes have been shown to be conducting or even superconducting.[20,21] Also, the neutral, odd-electron complex bis(benzene-1,2-dithiolato)gold(IV), **Ia**, has been isolated as semiconducting crystals with weakly dimerized one-dimensional stacks.[17,22] Furthermore, dithiolene complexes—especially the planar Ni- and Cu-group bis(dithiolenes)—presently attract considerable attention because of their third-order nonlinear optical properties.[23−30]

In relation to the electronic structure of dithiolene complexes, attention has hitherto focused on complexes of the early transition metals; especially the Ni dithiolenes. Calculations as well as experimental data, however, suggest close spacing of the valence orbitals in all dithiolene complexes of transition metals. The detailed ordering of valence orbitals consequently can be expected to vary with metal, ligand, and oxidation state.[9,10,34−40]

* To whom correspondence should be addressed.
† Centre for Interdisciplinary Studies for Molecular Interactions.
‡ Department of Chemistry.
§ Present address: Department of Solid State Physics, Risø National Laboratory, DK-4000 Roskilde, Denmark.
⊗ Abstract published in *Advance ACS Abstracts,* June 1, 1995.

(1) Gray, H. B. *Transition Met. Chem.* **1965**, *1*, 239.
(2) Livingstone, S. E. *Q. Rev. Chem. Soc.* **1965**, *19*, 386.
(3) McCleverty, J. A. *Prog. Inorg. Chem.* **1968**, *10*, 29.
(4) Eisenberg, R. *Prog. Inorg. Chem.* **1970**, *12*, 295.
(5) Hoyer, E.; Dietzsch, W.; Schroth, W. *Z. Chem.* **1971**, *6*, 41.
(6) Burns, R. P.; McAuliffe, C. A. *Adv. Inorg. Chem. Radiochem.* **1979**, *22*, 303.
(7) Mahadevan, C. *J. Crystallogr. Spectrosc. Res.* **1986**, *16*, 347.
(8) Davison, A.; Edelstein, N.; Holm, R. H.; Maki, A. H. *Inorg. Chem.* **1963**, *2*, 1227.
(9) Williams, R.; Billig, E.; Waters, J. H.; Gray, H. B. *J. Am. Chem. Soc.* **1966**, *88*, 43.
(10) Baker-Hawkes, M. J.; Billig, E.; Gray, H. B. *J. Am. Chem. Soc.* **1966**, *88*, 4870.
(11) Davison, A.; Howe, D. V.; Shawl, E. T. *Inorg. Chem.* **1967**, *6*, 458.
(12) Waters, J. H.; Gray, H. B. *J. Am. Chem. Soc.* **1965**, *87*, 3534.
(13) Van Rens, J. G. M.; Viegers, M. P. A.; DeBoer, E. *Chem. Phys. Lett.* **1974**, *28*, 104.
(14) Schlupp, R. L.; Maki, A. H. *Inorg. Chem.* **1974**, *13*, 44.
(15) Jenkins, J. J. Thesis, Howard University, 1976.
(16) Schultz, J.; Wang, H. H.; Soderholm, L. C.; Sifter, T. L.; Williams, J. M.; Bechgaard, K.; Whangbo, M. *Inorg. Chem.* **1987**, *26*, 3757.
(17) Rindorf, G.; Thorup, N.; Bjørnholm, T.; Bechgaard, K. *Acta Crystallogr.* **1990**, *C46*, 1437.
(18) Schiødt, N. C.; Bjørnholm, T.; Jacobsen, C. S.; Bechgaard, K. *Synth.Met.* **1993**, *56*, 2164.
(19) Yagubskii, E. B.; Kotov, A. I.; Laukhina, E. E.; Ignatiev, A. A.; Buravov, L. I.; Khomenko, A. G.; Shklover, V. E.; Nagapetyan, S. S.; Struchkov, Yu. T. *Synth. Met.* **1991**, *42*, 2515.
(20) Ibers, J. A.; Pace, L. J.; Martinsen, J.; Hoffman, B. M. *Struct. Bonding* **1982**, *50*, 1.
(21) Brossard, L.; Bousseau, M.; Ribault, M.; Valade, L.; Cassoux, P. *C. R. Acad. Sci. Paris* **1986**, *302*, 205.
(22) Schiødt, N. C.; Bjørnholm, T.; Neumeier, J. J.; Schilling, J. J.; Allgeier, C.; Jacobsen, C. S.; Thorup, N.; Bechgaard, K. Submitted for publication in *Phys. Rev. B.*
(23) Winter, C. S.; Oliver, S. N.; Rush, J. D.; Hill, C. A. S.; Underhill, A. E. *J. Appl. Phys.* **1992**, *71*, 512.
(24) Winter, C. S.; Oliver, S. N.; Manning, R. J.; Rush, J. D.; Hill, C. A. S.; Underhill, A. E. *J. Mater. Chem.* **1992**, *2*, 443.
(25) Oliver, S.; Winter, C. *Adv. Mater.* **1992**, *4*, 119.
(26) Fukaya, T.; Mizuno, M.; Murata, S.; Mito, A. *Proc. SPIE—Int. Soc. Opt. Eng.* **1992**, SPIE Vol. 1626, 135.
(27) Kafafi, Z. H.; Lindle, J. R.; Flom, S. R.; Pong, R. G. S.; Weisbecker, C. S.; Claussen, R. C.; Bartoli, F. J. *Proc. SPIE—Int. Soc. Opt. Eng.* **1992**, SPIE Vol. 1626, 135.
(28) Hill, C. A. S.; Underhill, A. E.; Charlton, A.; Winter, C. S.; Oliver, V.; Rush, J. D. *Proc. SPIE—Int. Soc. Opt. Eng.* **1992**, SPIE Vol. 1775, 43.
(29) Craig, B. I.; Williams, G. R. J. *Appl. Phys. B* **1993**, 56, 331.
(30) Bjørnholm, T.; Geisler, T.; Petersen, J. C.; Greve D.; Schiødt, N. C. *Nonlinear Opt.*, in press.
(31) Schrauzer, G. N. *Transition Met. Chem.* **1968**, *4*, 299.
(32) Schrauzer, G. N. *Acc. Chem. Res.* **1969**, *2*, 72.
(33) Herman, Z. S.; Kirchner, R. F.; Loew, G. H.; Mueller-Westerhoff, U. T.; Nazzal, A.; Zerner, M. C. *Inorg. Chem.* **1982**, *21*, 46.
(34) Chandramouli, G. V . R.; Manoharan, P. T. *Inorg. Chem.* **1986**, 25, 4680.

0020-1669/95/1334-3688$09.00/0

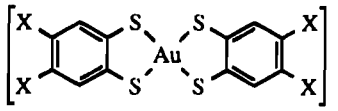

I: X = H, II: X = CH_3, III: X = SCH_3, IV: X = OCH_3, V: X = $(SCH_2CH_2S)_{1/2}$, VI: X = $(OCH_2CH_2O)_{1/2}$, VII: X = $(SC(S)S)_{1/2}$, VIII: X = $(SC(O)S)_{1/2}$

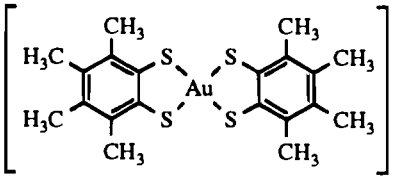

IX

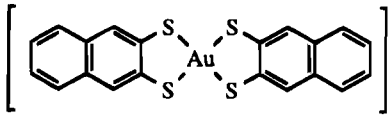

X

Figure 1. Compounds used in the present study. The roman numbers refer to the anionic complexes or their *n*-Bu_4N^+ salts. Neutral gold dithiolenes will be labeled by the corresponding roman number followed by **a**.

The intense, near-infrared absorption band for the structurally similar Ni–bis(dithiolene) complexes (both neutral and monoanionic) is known to be sensitive to ligand variation and has therefore been assigned as a (mainly) ligand-based $\pi-\pi^*$ transition.[10,31–33] Though occurring with a much smaller intensity, near-IR bands are also observed in the single-crystal[34] and solution[34–36] optical spectra of the dianionic species $((n\text{-}Bu_4N)_2(Ni(mnt)_2)$. Such near-IR bands are completely absent in the spectra of monoanionic Au–bis(dithiolene) complexes. However, we found that the Au complexes have two broad, weak absorption peaks in the visible region which are also sensitive to substituents on the ligand. While there have been numerous calculations of the electronic structure of the Ni complexes, very little attention has been paid to the Au dithiolenes.

We wished to obtain a detailed picture of the electronic structure in the valence region of the gold–dithiolene complexes, hoping for a better understanding of the relationship between certain physical properties such as molecular second order hyperpolarizability and conductivity of molecular crystals and the electronic structure in transition metal dithiolene complexes. Thus, we have measured the visible absorption maxima and the potentials of the reversible oxidation (when obtainable) for a series of monoanionic, aromatic Au–bis(dithiolene) complexes differing only in the substituents on the aromatic part of the ligand. These experimental data have been compared to the *ab initio* calculations on the "parent" complex of this series: bis(benzene-1,2-dithiolato)aurate(1–), **I**, and on the one-electron-oxidation product of this species, **Ia**. The complexes discussed in this paper are shown in Figure 1.

Experimental Section

a. Synthesis of Aromatic *o*-Dithiols. The ligands of the complexes **III**, **V**, **VII**, and **VIII** were prepared according to the method given by Larsen and Bechgaard,[41] and the synthesis of benzene-1,2-dithiol was performed by following Testaferri et al.[42] The remaining ligands were synthesized from the corresponding aromatic *o*-dibromides by reaction with cuprous alkanethiolate followed by reductive cleavage of the alkyl–sulfur bond with sodium in liquid ammonia. Different variations of this method appear in the literature,[43–48] but we found it essential to modify the published procedure for the first step. The following method worked well: A 10 mmol sample of the aromatic *o*-dibromide (e.g. 1,2-dimethyl-4,5-dibromobenzene for the preparation of 1,2-dimethylbenzene-4,5-dithiol) was dissolved in 20 mL of DMF. A 4 mL portion of pyridine was added together with 11 mmol of Cu_2O and 22 mmol of propane-2-thiol. The stirred suspension was then brought to vigorous reflux under a stream of N_2 for 24 h. The resulting brown solution was cooled to room temperature and poured into a mixture of 200 mL of aqueous ammonia and 10 g of NH_4Cl. While this mixture was well-stirred, 1 mL of 30% H_2O_2 was added, giving rise to immediate intensification of the blue color. The solution was immediately extracted with three 100 mL portions of diethyl ether. The combined extracts were washed with water, twice with dilute hydrochloric acid, and then again with water. After the etheral solution was dried, the solvent was evaporated, leaving a yellowish oil (obtained in 55–88% yield). This could be distilled *in vacuo* or in some cases induced to crystallize. However, 90 MHz ^1H NMR showed these raw products to be fairly pure and no further purification was necessary before the following reduction. After cleavage of the bis(sulfides) to the bis(dithiols) (according to the literature[43–48]), the identity of the ligands was checked by means of melting point, microanalysis, and ^1H NMR, and these physical properties were found to be in accordance with published data.

b. Synthesis of Aromatic Dithiolene Complexes of Au(III), Isolated as *n*-Bu_4N^+ Salts. The ligand (2 mmol) was dissolved in 25 mL of deoxygenated, absolute ethanol together with 4 mmol of hydrated sodium acetate. While this solution was well-stirred under nitrogen, a solution of 1 mmol of $Na(AuCl_4)$ in 50 mL of the same solvent was slowly added. The characteristic green color developed immediately, but at a certain point in the addition of the gold chloride solution (50–100% of the theoretical amount) a brown precipitate formed. The addition was stopped at this point, the solution was filtered, and 1.2 mmol of *n*-Bu_4NBF_4 dissolved in ethanol (10 mL) was added. Whether a precipitate formed immediately or not, the solution/suspension was stored at 5 °C overnight. The green or golden-green crystals were filtered off, and washed successively with ethanol and diethyl ether, air-dried, and recrystallized from CH_2Cl_2, $CHCl_3$, or mixtures of these solvents with diethyl ether, as indicated in Table 1 for the individual compounds. Included in Table 1 are melting points and elemental compositions as found by microanalysis.

c. Cyclic Voltammetry. The voltammetric cell, the electrodes (working electrode: 0.6 mm polished platinum), and the electrochemical instrumentation have previously been described.[49] Cyclic voltammetry was carried out in *N,N*-dimethylformamide, DMF (Ferak), which was distilled at reduced pressure prior to use. *n*-Bu_4NPF_6 (0.07–0.10 M) was used as supporting electrolyte. The formal potentials for **I–X/Ia–Xa** were determined as $E^{o\prime} = (E_{ox}^{p} + E_{red}^{p})/2$, where E_{ox}^{p} and E_{red}^{p} refer to the peak potentials for the oxidation and reduction processes, respectively. The peak potentials were read directly from the oscilloscope in XY-mode, and at each sweep rate an average of at least

(35) Schrauzer, G. N.; Mayweg, V. P. *J. Am. Chem. Soc.* **1965**, *87*, 3585.
(36) Shupack, S. I.; Billig, E.; Clark, R. J. H.; Williams, R.; Gray, H. B. *J. Am. Chem. Soc.* **1964**, *86*, 4594.
(37) Zalis, S.; Vlcek, A. A. *Inorg. Chim. Acta* **1982**, *58*, 89.
(38) Ciullo, G.; Sgamellotti, A. *Z. Phys. Chem. (Munich)* **1976**, *100*, 67.
(39) Alvarez, S.; Vicente, R.; Hoffmann, R. *J. Am. Chem. Soc.* **1985**, *107*, 6253.
(40) Sano, M.; Adachiu, H.; Yamatera, H. *Bull. Chem. Soc. Jpn.* **1981**, *54*, 2636.
(41) Larsen, J.; Bechgaard, K. *J. Org. Chem.* **1987**, *52*, 3285.
(42) Testaferri, L.; Tiecco, M.; Tingoli, M.; Chianelli, D.; Montanucci, M. *Synthesis* **1983**, 751.
(43) Gleiter, R.; Uschmann, J. *J. Org. Chem.* **1986**, *51*, 370.
(44) Adams, R.; Reifschneider, W.; Nair, M. D. *Croat. Chem. Acta* **1957**, *29*, 277.
(45) Adams, R.; Ferretti, A. *J. Am. Chem. Soc.* **1959**, *81*, 4927.
(46) Adams, R.; Reifschneider, W.; Ferretti, A. *Organic Syntheses;* Wiley: New York, 1973; Collect. Vol. V, p 107.
(47) Ferretti, A. *Organic Syntheses;* Wiley: New York, 1973; Collect. Vol. V, p 419.
(48) Wölki, N.; Klar, G. *Phosphorus Sulfur Relat. Elem.* **1988**, *36*, 261.
(49) Folmer Nielsen, M.; Laursen, S. Aa.; Hammerich, O. *Acta Chem. Scand.* **1990**, *44*, 932.

Table 1. Analytical Data for the Complexes

	yield (%)	mp (°C)	anal.: found (calc) % C	% H	% N	% S	% Au
I	54	184[b]	46.92 (46.72)	6.35 (6.16)	1.95 (1.95)		27.4 (27.4)
II	72	225[c]	49.23 (49.53)	6.76 (6.75)	1.78 (1.80)	16.38 (16.53)	26.1 (25.4)
III	49	235−7[a,b]	42.10 (42.50)	5.91 (5.81)	1.57 (1.55)		21.6 (21.8)
IV	38	238[a,d]	45.56 (45.76)	6.28 (6.24)	1.60 (1.67)	14.97 (15.27)	24.2 (23.4)
V	31	243−4[d]	42.62 (42.70)	5.30 (5.37)	1.46 (1.56)		21.8 (21.9)
VI	50	247−9[a,b]	45.96 (45.98)	5.77 (5.79)	1.64 (1.68)		23.6 (23.6)
VII	56	226−7[a,c]	38.78 (38.65)	4.40 (4.32)	1.48 (1.50)	34.30 (34.39)	21.3 (21.1)
VIII	31	201−3[e]	40.08 (40.03)	4.55 (4.48)	1.57 (1.56)	28.20 (28.50)	22.3 (21.9)
IX	80	259−60[d]	52.64 (51.96)	7.55 (7.27)	1.92 (1.68)	16.06 (15.41)	22.6 (23.7)
X	33	255−7[a,c]	52.57 (52.73)	5.60 (5.90)	1.83 (1.71)		

[a] Decomposes. [b] Crystallized from $CHCl_3/Et_2O$. [c] Crystallized from CH_2Cl_2. [d] Crystallized from CH_2Cl_2/Et_2O. [e] Crystallized from $CHCl_3$.

Table 2. Reversible Potentials[a] *vs* Fc/Fc^+, Visible Absorption Maxima, and Molar Extinction Coefficients[f]

	$E^{\circ\prime}$ (mV)	S conc (mM)	$\tilde{\nu}_1$ (ϵ_1) (eV ($M^{-1}cm^{-1}$))	$\tilde{\nu}_2$ (ϵ_2) (eV ($M^{-1}cm^{-1}$))
I	365	1.11	1.94 (70)	2.94 (190)
II	215	1.08	1.88 (80)	2.85 (185)
III	245	0.66	1.86 (120)	2.85 (250)
IV	60	0.60	1.77 (90)	*g*
V	255[b]	0.53	1.88 (110)	2.82 (325)
VI	145	0.89	1.83 (100)	2.77 (185)
VII	430[c]	0.34	1.95 (190)	*h*
VIII	285[c]	0.96	1.92 (100)	2.87 (260)
IX	125[d]	1.11	2.01 (75)	3.03 (735)
X	510[e]	1.15	2.09 (135)	2.77 (420)

[a] In DMF (0.07−0.10 M n-Bu_4NPF_6) at Pt electrode (0.6 mm) at v = 100 V s^{-1}; $\Delta E^{\circ\prime}$ = ±5 mV. [b] Not fully reversible, v = 1000 V s^{-1}. [c] Tabulated value is E_{ox}^{p} at 100 V s^{-1} since chemical reversibility was not obtained even at 1000 V s^{-1}. [d] v = 500 V s^{-1}. [e] Not fully reversible, v = 2000 V s^{-1}; $\Delta E^{\circ\prime}$ = ±20 mV in this case. [f] In CH_2Cl_2 (1 mM). [g] The λ_2 absorption peak was obscured by a third transition in this region. [h] The λ_2 absorption was hidden by very intense ligand absorptions.

three measurements was taken. When possible (see Results and Discussion), $E^{\circ\prime}$ was determined at several sweep rates, giving values identical within ± 5 mV. At v = 100 V s^{-1} the peak separation was typically on the order of 100 mV. Ferrocene (Fc, Fluka) was used as internal standard, and the potentials in Table 2 are given relative to Fc/Fc^+.

d. Electronic Spectra. The electronic spectra of the n-Bu_4N^+ salts **I**−**X** were recorded in methylene chloride solution (HPLC grade, previously dried by passing it through basic alumina) on a Hewlett Packard 8452A diode array spectrophotometer. Attention was focused on the relatively weak transitions in the visible region. The absorption maxima and molar extinction coefficients were measured twice (on different samples); see Table 2.

Results and Discussion

a. Calculations. *Ab initio* calculations were performed on **I** and **Ia** using a double-ζ basis set with core pseudopotentials (LANL1DZ) using an SCF−HF calculation.[50−52] The program Gaussian 90 was used.[53] The input was in both cases the bond lengths and bond angles as determined by X-ray analysis[17] of **Ia** averaged in such a way as to obtain D_{2h} symmetry, which is very close to the actual geometry of this compound. This geometry was not optimized prior to the calculations on **I** since the bond distances are not very different in the reduced and oxidized forms, as judged from a comparison between the X-ray data on **Ia** and the compound n-$Bu_4NAu(tdt)_2$,[54] which is very similar to **I** (tdt^{2-} = toluene-3,4-dithiolate). The results are given in schematized form in Figure 2B referring to the coordinate system shown in Figure 2A. The calculation on the doublet **Ia** gave rise to the same ordering of orbitals as the calculations on **I** with only small differences in coefficients on the atoms but quite large differences in the energy of the levels. The energies in **Ia** are for the α-electrons (the ground state population comprises 58 α-electrons and 57 β-electrons). A CIS calculation (configuration interaction with single excitations) was made on **I**, considering the three lowest lying excitations. This resulted in the prediction of three symmetry-forbidden transitions at 2.44, 3.68, and 3.73 eV, respectively, where the first of these is primarily a HOMO → LUMO transition (HOMO and LUMO refer to the orbitals in Figure 3). The first excited state is of B_{3g} symmetry, and the pure HOMO → LUMO configuration enters the linear combination with a coefficient of 0.67. The second and third excitations are nearly equal in energy, and they are primarily a HOMO-1 → LUMO and a HOMO-2 → LUMO transition (HOMO-1 refers to the second highest occupied molecular orbital etc.). The second excited state is of A_u symmetry, and the pure HOMO-1 → LUMO configuration enters the linear combination with a coefficient of 0.68. The third excited state is of B_{2g} symmetry with more mixed coefficients. The calculated transition energies are somewhat higher than the two measured absorptions (1.94 and 2.94 eV, respectively; see Table 2), but this is to be expected when the CI is not more elaborate than is the case here. However, both transitions are symmetry-forbidden in accordance with the calculation since in D_{2h} symmetry x transforms as b_{3u}, y as b_{2u}, and z as b_{1u}. The four previously mentioned MO's are depicted in Figure 3 with coefficients of the basis functions outlined (only indicated if numerically larger than 0.05, except for the LUMO, where the limit was placed at 0.1). The D_{2h} symmetry gives the coefficients for nonlabeled atoms.

It is of interest to compare the nature and ordering of the valence orbitals of **I** and **Ia** with those of similar Ni−dithiolenes, and this is done in the following where attention has be focused on the complexes $Ni(mnt)_2^{2-}$, $Ni(mnt)_2^-$, and $Ni(S_2C_2H_2)_2$, mnt^{2-} being malononitriledithiolate dianion. These species have been thoroughly examined experimentally and have been the subject of recent calculations. The state of the art regarding the sequence of energy levels in $Ni(mnt)_2^{2-}$ has been summarized by Chandramouli and Manoharan and an orbital energy diagram—consistent with their own detailed optical spectral

(50) Hay, P. J.; Wadt, W. R. *J. Chem. Phys.* **1985**, *82*, 270.
(51) Wadt, W. R.; Hay, P. J. *J. Chem. Phys.* **1985**, *82*, 284.
(52) Hay, P. J.; Wadt, W. R. *J. Chem. Phys.* **1985**, *82*, 299.
(53) Frisch, M. J.; Head-Gordon, M.; Trucks, G. W.; Foresman, J. B.; Schlegel, H. B. ; Raghavachari, K.; Robb, M. A.; Binkley, J. S.; Gonzales, C.; Defrees, D. J.; Fox, D. J.; Whiteside, R. A.; Seeger, R.; Melius, C. F.; Baker, J.; Martin, R. L.; Kahn, L. R.; Stewart, J. J. P; Topiol, S.; Pople, J. A. *Gaussian 90*; Gaussian Inc.: Pittsburgh, PA, 15213, 1990.
(54) Mazid, M. A.; Razi, M. T.; Sadler, P. J. *Inorg. Chem.* **1981**, *20*, 2872.

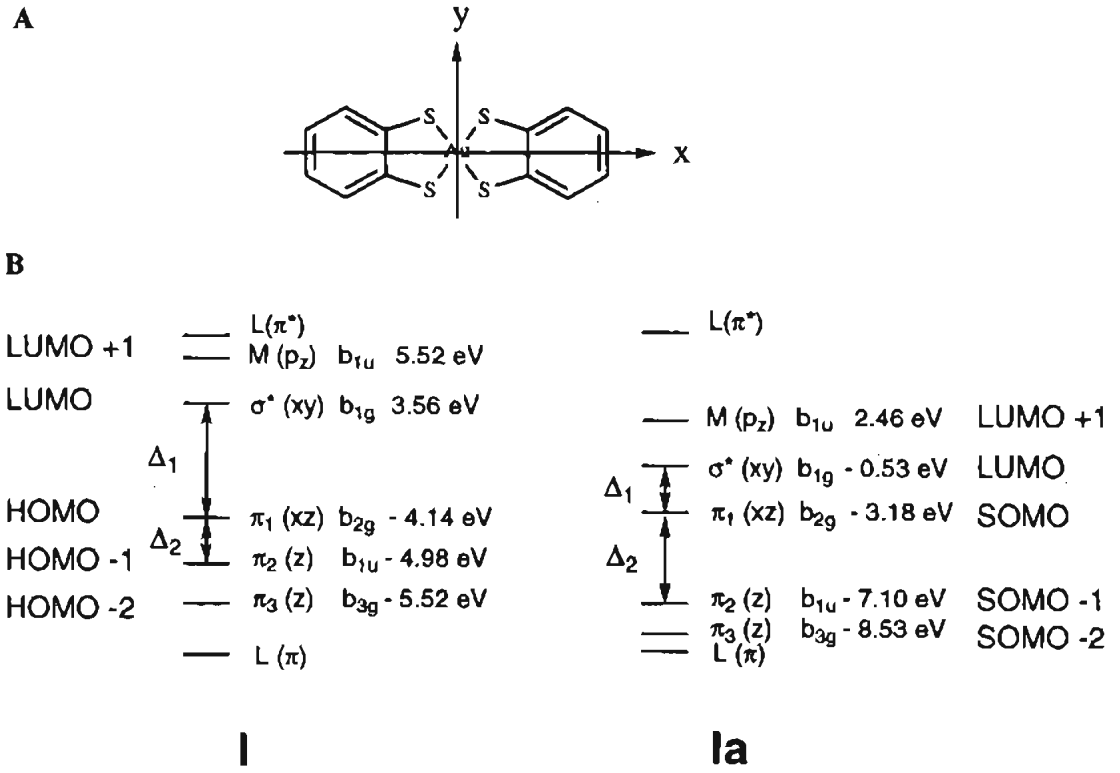

Figure 2. (A) Coordinate system used for the *ab initio* calculations and (B) the electronic structure in the valence region of **I** (left) and **Ia** (right).

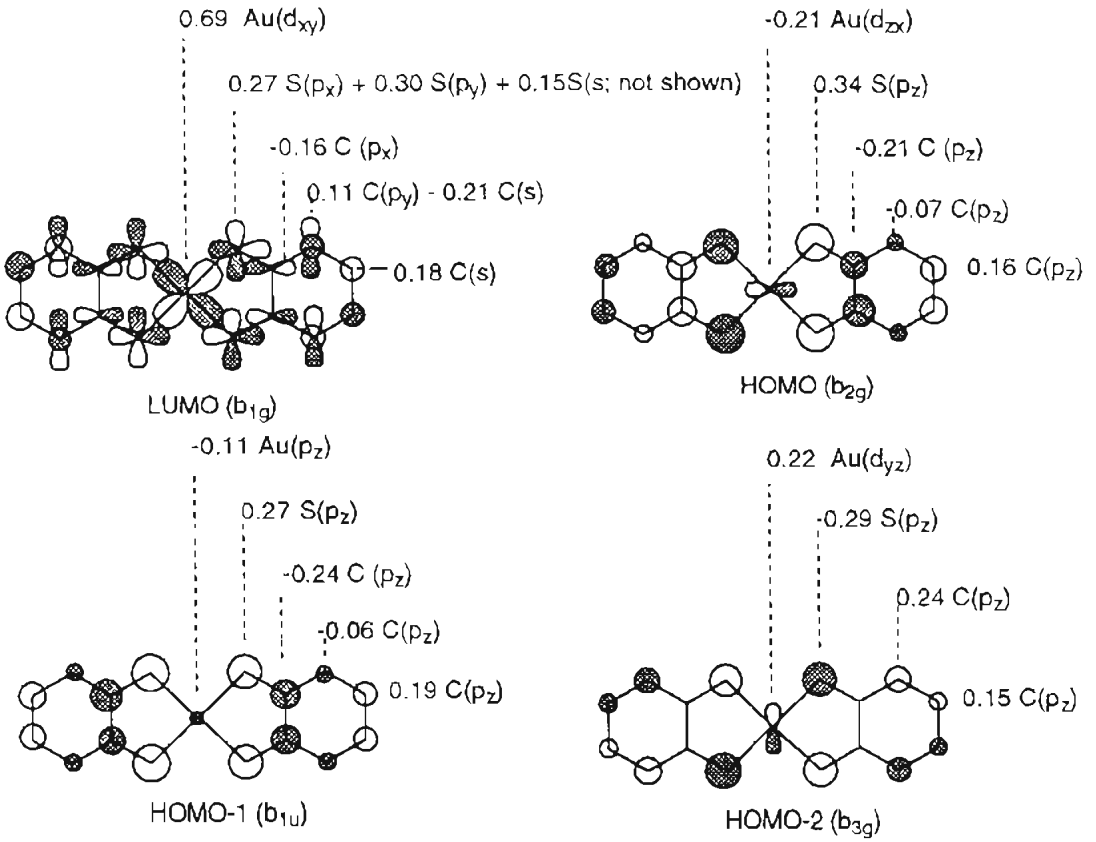

Figure 3. Coefficients on the basis functions in some of the valence MO's according to the *ab initio* calculations on **I**.

studies in solution and in single-crystal media—has been proposed.[34] Discrete variational Xα calculations on this complex and on the monoanion $Ni(mnt)_2^-$ have been performed[40] by Sano et al. Finally, Herman et al. have reported an INDO-type LCAO–MO–CI calculation on bis(ethylene-1,2-dithiolato)nickel ($Ni(S_2C_2H_2)_2$) supported by optical solution spectra.[33]

The LUMO and the three highest occupied molecular orbitals of **I** shown in Figure 3 appear in order of decreasing energy as

$$b_{1g}(\sigma^*, 48\%\ 5d_{xy}) > b_{2g}(\pi^*, 4\%\ 5d_{xz}) > b_{1u}(\pi) > b_{3g}(\pi)$$

The d orbitals in **I** other than d_{xy} were found at rather low energies. If the "% d orbital character" of an MO is considered

as the squared coefficient of the d orbital in this MO, the following sequence arises (considering only MO's with >20% M character): orbital no. 59—LUMO—(b_{1g}) 48% d_{xy}; 44 (a_g) 30% $d_{x^2-y^2}$; 41 (b_{1g}) 22% d_{xy}; 38 (b_{3g}) 81% d_{xz}; 36 (a_g) 40% d_{z^2}; 35 (b_{2g}) 71% d_{xz}; 32 (a_g) 31% d_{z^2}, 23% $d_{x^2-y^2}$. Consider now the species $Ni(mnt)_2^{2-}$, which is valence-isoelectronic with **I**. The sequence proposed in ref 34 is—starting from the LUMO—as follows

$$b_{1g}(3d_{xy}) > b_{2g}(L + 3d_{xz}) > a_g(3d_{x^2-y^2}) > b_{1u}, b_{2u}, b_{3u}, b_{1g}(L)$$

and for the same complex from ref 40 (starting from the HOMO since the LUMO was not considered and transferring the representations to the coordinate system of Figure 2A)

$$b_{2g}(L, 28.5\%\ 3d_{xz}) > b_{3g}(60.5\%\ 3d_{yz}), a_g(85\%\ 3d_{x^2-y^2})$$

and from the same reference for $Ni(mnt)_2^-$ (here given as the value of the α electrons)

$$b_{2g}(L, 17.9\%\ 3d_{xz}) > b_{3g}(48.9\%\ 3d_{yz}), b_{1u}(L), a_g(81.5\%\ 3d_{x^2-y^2})$$

In the neutral $Ni(S_2C_2H_2)_2$ from ref 33 the sequence is (starting from LUMO + 1)

$$b_{1g}(\sigma^*, 52\%\ 3d_{xy}) > b_{2g}(\pi^*, 16\%\ 3d_{xz}) > b_{1u}(\pi) > b_{3g}(\pi, 28\%\ 3d_{yz})$$

As can be seen, the frontier orbitals in **I** (and **Ia**, which has the same sequence) LUMO and HOMO (SOMO in **Ia**) have the same symmetry as the comparable orbitals in the three nickel complexes. A main feature of the spectra of neutral and monoanionic Ni—bis(dithiolene) complexes (and their Pd and Pt analogs as well) is the intense, allowed substituent-dependent near-IR transition. This is generally considered to be principally the HOMO—LUMO $\pi-\pi^*$ transition ($b_{1u}-b_{2g}$). This band is absent in the spectrum of **I** since the b_{2g} orbital has become doubly occupied. The oxidized species **Ia** is a black, semiconducting, crystalline solid with intense near-IR absorptions. Unfortunately, we have not been able to dissolve this compound without reaching the decomposition point and therefore we are unable to distinguish molecular transitions from intermolecular band transitions (see note added in proof).

A general feature of the above orbitals is the larger amount of metal character in the valence orbitals of the Ni species as compared to **I**. This is to be expected, since the heavier transition metals in general form bonds with a higher degree of covalency than do the early transition metals and since the ligands in **I** are more conjugated and more electron donating than the ligands of the nickel complexes referred to above. A very interesting consequence of the nearly absent metal character in the SOMO of **Ia** is the almost complete lack of dimerization in the solid state in strong contrast to salts of $Ni(mnt)_2^-$. This ion has been shown[55] to dimerize in the solid state by coordination of each Ni in the dimer by a sulfur atom in the other molecule of the dimer so as to obtain five-coordinate Ni. This possibility is prohibited in the case of **Ia** since no orbitals centered on the gold atoms suitable for overlap in this way are available. The SOMO is delocalized on the ligands and will not be expected to be able to form a strong bond.

(55) Kuppusamy, P.; Manahavan, C.; Mahadevan, C.; Seshasayee, M. *J. Crystallogr. Spectrosc. Res.* **1985**, *15*, 359.

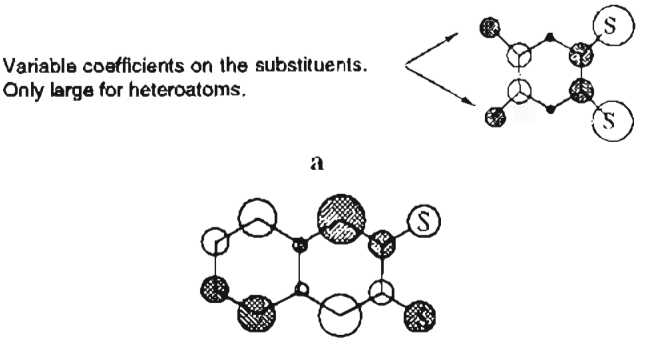

Figure 4. Schematic representation of (a) HOMO of the free ligands from complexes **I** through **IX** and (b) HOMO of naphthalene-2,3-dithiol.

MNDO calculations were performed on the 10 ligands (as protonated, neutral species) using the program MOPAC 4.2.[56] The HOMO on the free ligands was found to have the appearance shown in Figure 4a for the ligands in complexes **I**—**IX**, while that of naphthalene-2,3-dithiol (the ligand in complex **X**) was found to be quite different (Figure 4b).

b. Electronic Spectra. The complexes all had two weak, broad absorptions in the visible region. The energy at the absorption maxima (called $\mathcal{E}_1$ and $\mathcal{E}_2$, respectively) and the molar extinction coefficients (ϵ_1 and ϵ_2) are shown in Table 2. The order of magnitude of the molar extinction coefficients (see Table 2) indicates that the transitions are symmetry-forbidden, in agreement with the calculations. When the nature of these transitions is discussed in terms of the diagram in Figure 2B, it seems plausible that $\mathcal{E}_1$ corresponds to Δ_1 (the transition is mainly HOMO—LUMO) and $\mathcal{E}_2$ corresponds to $\Delta_1 + \Delta_2$ (mainly HOMO-1 to LUMO). When the aromatic dithiolene Au(III) complexes are arranged in order of increasing energy of $\mathcal{E}_1$, one obtains

$$\mathbf{IV} < \mathbf{VI} < \mathbf{III} < \mathbf{V} = \mathbf{II} < \mathbf{VIII} < \mathbf{I} < \mathbf{VII} < \mathbf{IX} < \mathbf{X}$$

with $\mathcal{E}_1$ varying from 1.77 eV for **IV** to 2.09 eV for **X**, a variation of 16.5% relative to the average $\mathcal{E}_1$. A somewhat different order is observed, when the series is based on the other transition, $\mathcal{E}_2$:

$$\mathbf{VI} < \mathbf{X} < \mathbf{V} < \mathbf{III} = \mathbf{II} < \mathbf{VIII} < \mathbf{I} < \mathbf{IX}$$

but when the structurally similar complexes (those substituted in the 4- and 5-positions only) are compared, the ordering is essentially the same, giving rise to the following "spectrochemical series" for the 4,5-substituted compounds (R is alkyl, Z is sulfur or oxygen):

$$C_6H_2S_2(OR)_2^{2-} < C_6H_2S_2(SR)_2^{2-} = C_6H_2S_2R_2^{2-} < C_6H_2S_2(S_2CZ)^{2-} = C_6H_2S_2H_2^{2-}$$

This sequence supports the previous assignment of $\mathcal{E}_1$ as a transition from a ligand π orbital (HOMO) to a mixed metal/ligand σ^* orbital (LUMO) since the energy of the former orbital would be expected to rise with increasingly electron releasing substituents while that of the latter would be expected to be rather insensitive to the substituents on the benzene ring. It is noteworthy that according to this scheme $\mathcal{E}_1$ can be looked upon as a symmetry-forbidden ligand to metal charge transfer (LMCT) transition. This will be further elaborated in the following section.

(56) Stewart, J. J. P. *QCPE* **1987**, No. 455.

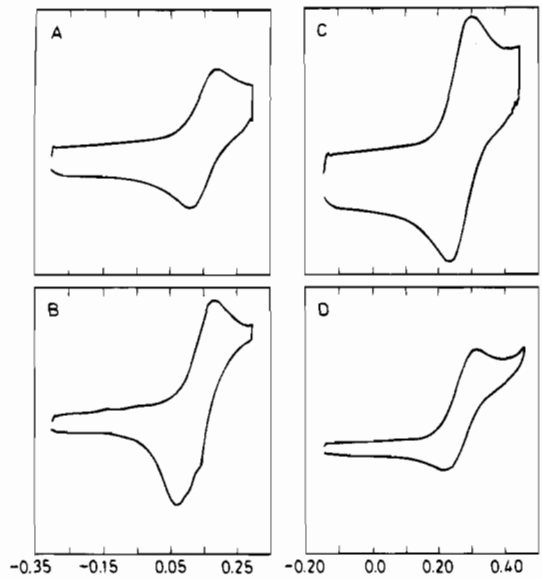

Figure 5. (A, B) Cyclic voltammograms of **VI** in DMF (0.1 M n-BuNPF$_6$) at a Pt electrode (d = 0.6 mm). Potentials are in V vs Fc/Fc$^+$. Scan rate: v = 50 V s^{-1} (A); v = 5 V s^{-1} (B). (C, D) Cyclic voltammograms of **I** in DMF (0.1 M n-BuNPF$_6$) at a Pt electrode (d = 0.6 mm). Potentials in V vs Fc/Fc$^+$. Scan rate: v = 100 V s^{-1} (C) , v = 10 V s^{-1} (D).

c. Cyclic Voltammetry. Cyclic voltammetry (CV) of complexes **I**−**X** in DMF in all cases showed an oxidation peak in the potential range 0−0.6 V *vs* the ferrocene/ferrocenium redox couple (Fc/Fc$^{\bullet+}$). The stability of the neutral species formed upon oxidation varied from complex to complex as estimated by the sweep rate, v, necessary to obtain chemical reversibility. For complex **VI** chemical reversibility was obtained at v = 50 V s^{-1} as shown in Figure 5A whereas for complex **I** v = 100 V s^{-1} was necessary (Figure 5C). At low sweep rates the initially formed product of the electrode reaction underwent a homogeneous follow-up reaction which resulted in a decrease in the reduction current on the reverse scan (Figure 5D) and was in some cases accompanied by the appearence of a new reduction peak at a lower potential due to a product of the follow-up reaction. In the case of complex **VI**, this additional peak appears as the main reduction peak in the voltammogram at v = 5 V s^{-1} in Figure 5B.

The values of the potentials for the reversible oxidations in Table 2 were calculated as the midpoint between the oxidation and reduction peak potentials at v = 100 V s^{-1} for the complexes **I**−**IV** and **VI**, while for **V**, **IX**, and **X** sweep rates of 1000, 500, and 2000 V s^{-1} were necessary to obtain chemical reversibility or partial chemical reversibility; cf. Table 2. Complexes **VII** and **VIII** showed chemically irreversible behavior even at v = 1000 V s^{-1}, the only reduction peaks observed being due to products of the follow-up reaction. Consequently, no formal potentials could be determined for these two compounds.

For structurally closely related donors the potentials for the reversible oxidation are expected to correlate linearly with the energies of charge transfer to a common acceptor[57] as well as with the vertical ionization potentials (IP) of the donors, if the reorganization and solvation energies ($\Delta G_r°$ and $\Delta G_s°$) are either constant or linearly related to the values of IP, eq 1. F is the

$$E^{\circ\prime} = \mathrm{IP} + (\Delta G_r^\circ + \Delta G_s^\circ)/F + \mathrm{const} \qquad (1)$$

(57) Masnovi, J. M.; Seddon, E. A.; Kochi, J. K. *Can. J. Chem.* **1984**, *62*, 2552.

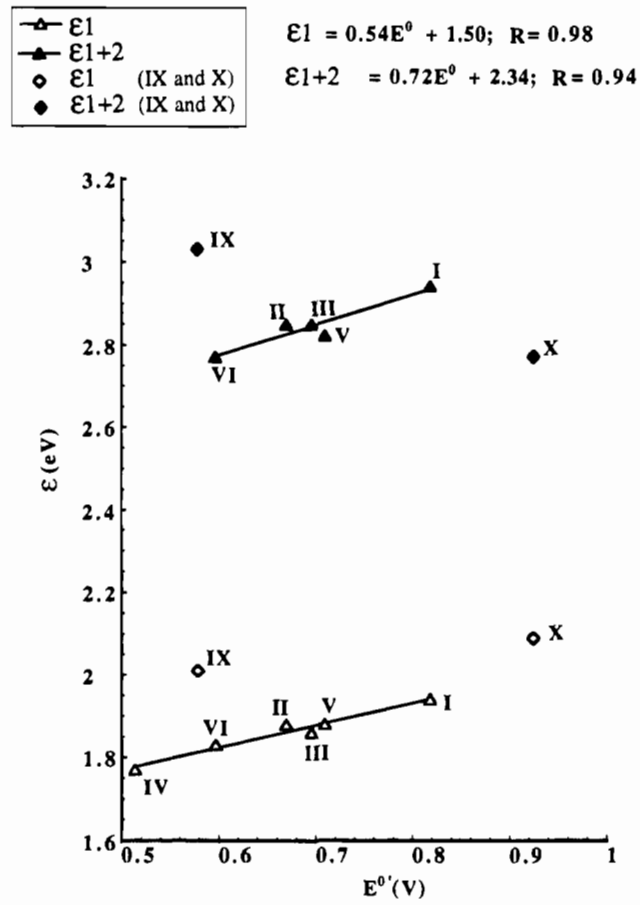

Figure 6. Correlation of absorption maximum energies ($\mathcal{E}_1$ and $\mathcal{E}_1$ + $\mathcal{E}_2$, respectively) with reversible potentials ($E^{\circ\prime}$) for the complexes. Reversible potentials were measured at 100 V/s except for **V** (1000 V/s), **IX** (500 V/s), and **X** (2000 V/s); see Table 2.

Farraday constant. For a series of 9- and 9,10-substituted anthracenes,[57] $E^{\circ\prime}$'s measured in solution by CV were found to be linearly related to experimentally determined IP's (eq 2) and charge transfer energies ($h\nu_{CT}$) involving the same donors and a common acceptor (eq 3).

$$\mathrm{IP} = 1.16E^{\circ\prime} + \mathrm{const} \qquad (2)$$

$$h\nu_{CT} = 0.82E^{\circ\prime} + \mathrm{const} \qquad (3)$$

In an analogous picture of the ligand to metal transitions, a correlation between the ligand to metal excitation energy and the value of $E^{\circ\prime}$ should be expected:

$$\mathcal{E}_1 = \mathrm{slope} \times E^{\circ\prime} + \mathrm{const} \qquad (4)$$

In the limit where the metal atom only provides a weak coupling between the ligands, the slope in eq 4 should be 1, since the ligand orbitals are affected by substitutions while the metal orbitals will be unaffected and hence fixed in energy. If, on the other hand, the coupling between the metal and ligand orbitals is strong, complete mixing of the states should be expected. The slope in eq 4 should be equal to ≈0 in this situation since both the metal and ligand states are affected by substitutions in a similar way.

In Figure 6 the values of $\mathcal{E}_1$ are plotted against the reversible potentials for the complexes where the latter was obtainable. The structurally similar complexes—those with 4,5-disubstituted benzenoid ligands—can be seen to follow a linear relation while compounds **IX** and **X** behave anomalously in this respect (this will be discussed below). In this case, the correlation between

the excitation energy and the reversible potential has a smaller slope (*ca.* 0.5) than that found for the system described by eq 3, indicating an intermediate situation between strong and weak coupling. Two results from the *ab initio* calculations corroborate this observation: (1) The transition can not be considered 100% HOMO−LUMO; other states are involved. (2) The LUMO is not constant in energy. The two major reasons for this are that this MO is about 50% ligand in character, and although it is a σ orbital, it cannot be considered completely "decoupled" from substitutions on the benzene ring.

Included in Figure 6 is also a plot of $\mathcal{E}_1 + \mathcal{E}_2$ vs $E^{\circ\prime}$. The same trend can be seen but with a somewhat smaller correllation coefficient (R).

Since the HOMO and HOMO-1 in complex **I** were found to be almost purely the antibonding and bonding combinations of the ligand HOMO's, the difference in the form of the ligand HOMO's in benzene- and naphthalenedithiols (Figure 4) could well account for the anomalously positioned absorption maxima in the electronic spectrum of **X**. The tetrasubstituted ligand of complex **IX** has two more electron-releasing methyl groups than **II**, but the absorption maxima of the former are significantly blue-shifted compared to those of all the complexes with 4,5-disubstituted ligands. Also, the molar extinction coefficient on $\mathcal{E}_2$ is strikingly larger than in any other of the measured compounds. These observations could well be due to a deviation from planarity of this complex, since the benzene ring is heavily substituted.

Conclusions

The MO picture provided by the *ab initio* calculations on **I** is well supported by the observed correlation of the energies of the two visible transitions with the potentials for the reversible oxidation of **I**−**VI**, since (assuming that introduction of substituents on the benzene ring in these positions will only imply minor perturbations of the MO diagram) the calculation predicts that the HOMO and HOMO-1 undergo a decrease in energy when going through the series from X = RO to X = H, while the LUMO is less affected. The MNDO calculations demonstrate that the ligand naphthalene-2,3-dithiol is electronically too different from its benzene analogue to make a direct comparison of **X** and **I** useful. In spite of its electron-releasing substituents, **IX** has absorption maxima at shorter wavelengths than any of the complexes with disubstituted ligands. It seems plausible, however, that this is due to a deviation from planarity in the complex because of the large steric demands from a hexasubstituted benzene. This explanation is supported by the large extinction coefficient of the ϵ_2 transition in this complex, since such would be expected if the geometry was distorted from D_{2h} symmetry.

A comparison of our *ab initio* calculations on **I** and **Ia** with recent calculations on similar Ni compounds[33,34,40] reveals many similarities between the orbitals in the valence region of these compounds, and the main differences and similarities concerning the spectral behavior of the gold and nickel dithiolenes can be understood in terms of the number of electrons involved and the electron-releasing nature of the ligands.

Acknowledgment. We wish to thank Ole Hammerich for the inspiring discussions and the Danish Material Research program for funding.

Note Added in Proof: Recently recorded near-IR reflectance spectra of a single crystal of **Ia** show two intense bands at 0.6 and 1.0 eV.[22] The band at 1.0 eV is intramolecular in origin and can thus be assigned as the expected $b_{1u} \rightarrow b_{2g}$ $\pi-\pi^*$ transition in analogy to the transition observed in monoanionic Ni−bis(dithiolene) complexes.

IC940237U